buildings

MDPI

Article

Automated Selection and Localization of Mobile Cranes in Construction Planning

Hongling Guo [1], Ying Zhou [1], Zaiyi Pan [1], Zhitian Zhang [1], Yantao Yu [2,*] and Yan Li [1]

[1] Department of Construction Management, Tsinghua University, Beijing 100086, China; hlguo@tsinghua.edu.cn (H.G.); zhouying17@mails.tsinghua.edu.cn (Y.Z.); pzy2456@126.com (Z.P.); zhangzt18@mails.tsinghua.edu.cn (Z.Z.); liyan1@cindata.cn (Y.L.)

[2] Department of Civil and Environmental Engineering, The Hong Kong University of Science and Technology, Hong Kong 999077, China

* Correspondence: ceyantao@ust.hk

Abstract: Accurate selection and location of mobile cranes is a critical issue on construction sites, being able to contribute to the improvement of the safety and efficiency of lifting operations. Considering the complexities and dynamics of construction sites, this study aimed to develop a useful approach for automated selection and localization of mobile cranes based on the simulation of crane operations. First, the information required for crane selection and localization is analyzed and extracted from BIM (building information modeling). Then, mainly considering the crane capacity, the initial crane type is selected with candidate location points. Based on the simulation of lifting operation at the candidate points, feasible location points and crane types are determined through three constraint checks (i.e., environment constraint, operation constraint, and safety constraint). Besides, two kinds of efficiency optimization, namely lifting time minimization and crane movement minimization, are presented to figure out the best location points from the feasible points. Finally, the proposed approach is validated using a case study. This research contributes to not only crane operation planning but also automatic construction simulation, thus supporting the implementation of intelligent construction in the future.

Keywords: mobile crane; automated selection; automated localization; virtual construction

check for updates

Citation: Guo, H.; Zhou, Y.; Pan, Z.; Zhang, Z.; Yu, Y.; Li, Y. Automated Selection and Localization of Mobile Cranes in Construction Planning. *Buildings* **2022**, *12*, 580. https://doi.org/10.3390/buildings12050580

Academic Editor: Lucio Soibelman

Received: 23 March 2022
Accepted: 27 April 2022
Published: 29 April 2022

Publisher's Note: MDPI stays neutral with regard to jurisdictional claims in published maps and institutional affiliations.

Copyright: © 2022 by the authors. Licensee MDPI, Basel, Switzerland. This article is an open access article distributed under the terms and conditions of the Creative Commons Attribution (CC BY) license (https://creativecommons.org/licenses/by/4.0/).

1. Introduction

As the most commonly used and shared site resources with large moving and heavy loads, mobile cranes are involved in all kinds of lifting works [1,2]. Considering the complication of hoisting, especially heavy weight lifting, a detailed hoisting scheme should be formulated before operation [3]. According to relevant statistics, the design of the hoisting scheme is a very important part of lifting work on construction sites, accounting for 60–80% of the whole lifting time [4]. It mainly includes crane selection, crane localization, and operation planning. However, the traditional hoisting scheme design mostly relies on the experience of site engineers, requiring a lot of two-dimensional (2D) drawings with limitations, such as a high error rate, low design efficiency, low safety level, and poor data synchronization. This calls for an urgent in-depth study to figure out the above critical problems.

In recent years, the rapid development of virtual construction and simulation technologies has provided a new solution. The application of virtual construction technology to the hoisting scheme design helps promote high-accuracy three-dimensional (3D) visualization, and advanced simulation and optimization. It is used extensively for the path planning of mobile cranes, training operators, or the detection of spatial conflicts [5–10]. Moreover, the simulated results further support the following crane selection or localization, respectively, especially the effects of different factors (i.e., wind effect [11], ground bearing pressure [12,13], rope breakage [14], and so on) on the operational feasibility. However,

crane selection and localization are essentially two mutually prerequisite steps that cannot be separated independently while previous research has treated them less as a whole process [15]. Due to the difference in the performance parameters between various types of cranes, not only the load but also the spatial relationship between a lifting object and a crane on a site should be considered to ensure that the selected crane meets the lifting requirements regarding the height and distance. Lifting collision is another indispensable problem in the selection of cranes. Moreover, mobile cranes can move to different locations on construction sites to meet the specific hoisting requirements mentioned above. Therefore, the hoisting scheme design needs to consider different location point combinations of lifting objects, minimizing the movement of the crane, and ensuring the safety of lifting processes.

Aimed at the above problems, this research aimed to develop a method to automatically select and locate mobile cranes in virtual construction to aid in hoisting scheme design. The rest of this paper is structured as follows. First, a literature review is outlined to analyze the limitations of current research in Section 2. Then, the research methodology is presented in Section 3. After that, the method for the automated selection and localization of mobile cranes is proposed in Section 4 and further tested based on a case study in Section 5. Finally, a conclusion is drawn in Section 6.

2. Literature Review

2.1. Crane Selection

Previous research on the selection of mobile cranes has mainly focused on the crane load and the distance between crane booms and buildings. Al-Hussein et al. [16] proposed a method to select a feasible crane by calculating whether the load of the crane and the gap between the crane and building components meet basic requirements based on independent 2D drawings involving a lot of manual input. Moselhi et al. [17] developed a selection and positioning system of a mobile crane to establish 3D models based on the coordinates and size of hoisting objects and obstacles and then simulated the position of the mobile crane and potential collisions in a virtual environment to identify the optimal crane. Based on the above research, a systematic method for the selection of mobile cranes was proposed [18]. It selected the optimal crane based on different constraints from feasible cranes that meet the minimum clearance with buildings, crane working radius, and crane load. For instance, the selection of a truss boom crane was optimized with the lifting radius while that of a hydraulic telescopic boom crane was achieved using the main boom length and working radius. Besides the crane load and safety distance, other factors, such as pressure and cost, have been considered in the selection of mobile cranes. For example, a study investigated the effect of the ground bearing pressure on the selection of a crane type by comparing the pressure of the crane on the ground with the ground bearing pressure [19]. Hasan et al. [20] calculated the pressure of each leg of a crane at different horizontal swing angles and ensured safety by checking the leg pressure during crane operation. Han et al. [21,22] considered the lifting capacity, working range, lifting height, and the first lifting weight to select a crane with the lowest cost in a feasible list of cranes. Furusaka and Gray [23] proposed an algorithm to realize the most economical combination of different cranes, with a new definition of the minimum total cost of a mobile crane, including leasing, assembly, and disassembly. Based on the feasible crane locations, Han et al. [24] proposed a 3D-based crane evaluation system to select the most suitable crane type under two circumstances (i.e., the fixed and unfixed crane), requiring module information inputs. Artificial intelligence (AI), on the other hand, has been used to select cranes in recent years. For example, the genetic algorithm (GA), as a heuristic random search technique, was used to determine the optimum location of a crane by considering safety, clearance, site conditions, etc. [25]. A discrete event simulation model was developed to realize the automatic planning of crane operation and the selection of the optimal crane type [26]. A system called PRECISE was developed to select the optimal crane type, which minimized the number of mobile crane operations [27].

The existing methods enable rapid calculation and analysis of the geometric and mechanical parameters of mobile cranes and construction sites, and realize the selection of the optimum crane for a specific construction project by considering several specific factors. Based on experience, this is more efficient and accurate than traditional methods. However, the selection methods in previous research mainly considered a 2D static environment. Although some methods have been combined with 3D models, they still need significant manual input or modeling [24]. In some studies, 3D modeling was even used as a visualization tool for animation demonstration after selection, which does not provide enough assistance in hoisting scheme design. Moreover, there is no comprehensive and systematic consideration of various factors, such as the site environment, operation, safety, and economy, in crane selection, with less consideration of the following progress (e.g., crane localization and path planning) [15].

2.2. Crane Localization

In terms of crane localization, three constraints (i.e., environmental constraint, operation constraint, and safety constraint) have mainly been considered in previous research. To deal with these constraints, different methods have been applied, which can be classified as the 2D-based method and the 3D simulation method. The 2D-based method uses mathematical formulas to calculate the feasible location areas or location points for a mobile crane. Although some methods consider spatial factors and establish 3D models, they are still based on the mathematical analysis of 2D drawings, thus being classified as a 2D-based method [28]. Lei [29] and Ding [30] obtained the appropriate location areas of a mobile crane by defining the outer boundary constraints of existing buildings or obstacles but without consideration of 3D spatial factors. Al-Hussein et al. [16] judged whether a crane satisfied the environmental constraints by comparing the building coordinates around the proposed location points and calculating the distance between the crane boom and the building. Considering that a crane should be located in the center of all buildings, Olearczyk et al. [3,4] proposed a method for calculating the geometric center coordinates of all buildings and analyzed the maximum working radius of a crane and the distance between its boom and the buildings to ensure the operability and safety of lifting work. Moreover, Hermann et al. [31] proposed another method to determine the location of mobile cranes in prefabricated building construction. First, a project manager defines a line and generates several random points on the line. Then, the distance between the center of each building and each random point is calculated to select the maximum distance for the random points, and finally, the above two steps are repeated to select the minimum distance from these maximum distances. The point with the minimum distance is the desired location point of the crane. Based on the 2D-based method, the feasible location area of the mobile crane is firstly obtained by considering its working radius or minimum operating distance. Then, other factors, including time and cost, are further considered to determine the optimal location point. However, this requires manual input of many parameters [32,33], which takes a significant amount of time, especially for complex spatial calculations. In addition, the accuracy of the obtained location points may be affected because some location points with collisions are not deleted while some feasible points are eliminated by mistake.

Considering the limitations of the 2D-based method, some research presents discrete simulation-based 3D methods [28,34–36]. Firstly, feasible location points are determined based on the construction environment and the reachability of cranes. Through simulation of the lifting operation, location points with spatial collisions or other unsatisfied constraints are deleted to obtain the optimal location points. Tantisevi et al. [28,34] selected feasible location points initially by judging the accessibility of a boom; screened out feasible location points using the bounding box, ray tracing algorithm, and conflict analysis method; and then obtained the optimal location points by traversing all operations of the crane with the minimization of crane relocalization. The first two steps of the method proposed by Wang et al. [35] are similar to those proposed by Tantisevi [28,34]. However, the

relocalization of the mobile crane is not considered while the total weight of a crane and lifting components is minimized from a safety perspective. In addition to the localization of an individual crane, some research has considered the operation of double cranes or multiple cranes. For example, Zi et al. [36] used a parallel robot method to solve the localization problem of multiple cranes based on the multi-point localization method and 3D grid method. Recently, integer programming [37,38] has been introduced to solve the location optimization problem of multiple cranes, with some assumptions disagreeing with reality, as limited by the computation resource.

Compared with the 2D-based method, the 3D simulation method not only considers spatial factors but also applies various simulation methods in spatial conflict analysis, making collision detection more dynamic and efficient. However, the changes in the lifting capacity during actual operations are not considered. The maximum load capacity of a mobile crane changes with the lifting radius. In addition, existing 3D simulation methods still require many manual inputs or modeling, neglecting the effect of other stages.

2.3. Research Gaps

As crane selection and localization are two interdependent processes [15], recently, some research [39–41] has attempted to consider the two processes simultaneously. Referring to the research gap that neglecting the impact of multiple construction stages leads to excessive costs, Yeoh and Chua [39] reframed crane selection and localization as a four-dimensional set cover problem (4D-SCP) to minimize the investment, with the limitation of static cranes. Focusing on multiple working cranes, Lin et al. [40] compared the working efficiency of different crane combinations to determine the optimal one with a value engineering model. However, collision detection, which is unavoidable between adjacent cranes, was considered less. Boo et al. [41] proposed a multi-objective optimization model for the selection of the tower crane number, types, and locations, which minimized cost and conflict, using a multi-objective optimization model. As a matter of fact, the calculation of the gap between a crane boom and an obstacle needs to consider the position of the boom in the elevation, and the existing selection algorithm inputs the crane location as a known item. Meanwhile, the determination of the crane location requires the information of the selected crane, which traps the calculation into a circular loop. Existing research does not take this iterative problem into account as a whole process. In addition, most of the relevant research only considers the hoist of a single component; however, it is a multi-component lifting process. Therefore, a method for automated selection and localization of mobile cranes is proposed in this research by combining the specification of the lifting operation and characteristics of mobile cranes with BIM (building information modeling) and virtual construction to ensure the safety, operability, and efficiency of lifting processes. Besides, the proposed method contributes to the automated simulation of construction processes, thus increasing the safety performance of lifting operations and reducing construction costs.

3. Methodology

Automated selection and localization of mobile cranes are two interdependent processes. As the first step of a hoisting scheme design, crane selection is based on the crane location and calculation to determine whether crane parameters meet the requirements. Therefore, this research regards the selection and localization of a mobile crane as a comprehensive planning process, taking both into consideration when analyzing the constraints and information requirements.

Figure 1 shows the process of automatically selecting and locating a mobile crane. Due to the complex environment of construction sites, the location of the mobile crane should meet the requirements of the site layout, that is, the environmental constraints. According to the construction plan, the plane range of an obstacle must be eliminated from the alternative location area. Then, the lifting requirements of the mobile crane, namely the operation constraints, including the transport distance, transport height, and the weight of

lifting objects, should be considered. Thirdly, safety constraints should be considered in the operation of the mobile crane. The selection and localization of the mobile crane can be simulated in a virtual environment to identify and remove collisions between booms and buildings. Once these constraints are analyzed, suitable crane types and feasible location points can be achieved. Traversing the generated alternative location points, the optimal combination of the crane type and location point can be determined. Moreover, time and cost are two important aspects of project management, and they should be analyzed and reduced through further optimization. On the one hand, a crane with a lower rental price is more advantageous when it meets the above constraints. On the other hand, relocation and lifting are two time-consuming activities in crane operation, and minimizing the relocation and lifting time can effectively reduce the total lifting time and improve the lifting efficiency. Aiming to meet the requirements of the constraints and optimization, the constraint conditions should be digitized first. The BIM model can be converted into relevant parameters, which describe the conditions, to support the automated selection and localization of the mobile crane through appropriate algorithms. The spatial structure of each component of a crane can be further simulated as well. Based on the process of automated selection and localization of the mobile crane, the key algorithms for the three constraints and efficiency optimization are developed and tested using a virtual experiment in the following sections.

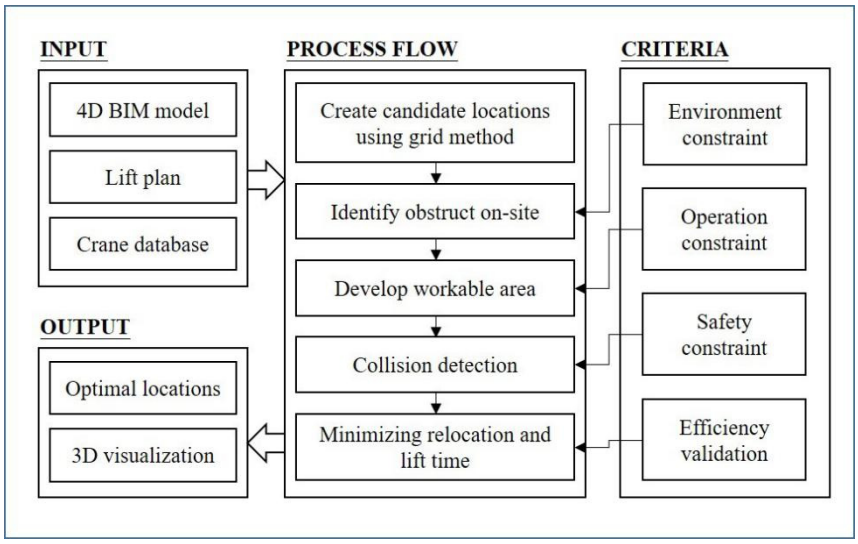


Figure 1. Logic framework of automated selection and localization of a mobile crane [42].

4. Method for Automated Selection and Localization of a Crane

4.1. Information Requirement and Extraction

The analysis of the above constraints and optimization requires a large amount of project information, most of which is contained in the 4D (four-dimensional) BIM model of a project. The 4D BIM model contains the specific location and external contour of the buildings and facilities on a construction site. This research takes prefabricated building construction as an example to explore the information requirements and extraction of crane selection and localization. For a prefabricated building, the lifting components usually involve walls, slabs, beams, etc. Relevant information can be obtained directly or indirectly from its IFC (Industry Foundation Classes) format BIM model. Table 1 displays the information regarding the building components that is extracted from the BIM model, which is required for crane selection and localization. Regarding the three constraints mentioned above, the information for each constraint is summarized in Table 2. Note that some information can be obtained directly while other information can be obtained through further calculation based on the parsed data from the BIM model, referring to our previous research [43,44]. In addition, the selection and localization calculation of a crane required

its performance parameters, which are stored in the crane database and are applicable to different construction projects. According to the above constraints and optimization, the required performance parameters are summarized in Table 3.

Table 1. Parameter information of building components for crane selection and localization.

Type	Position (x, y, z), $\vec{R}$	Size	Others
Wall	Vertical: starting position Horizontal: wall center line, core layer center line, surface layer center line, surface layer internal/external line, core layer internal/external line	Length L, Depth D, Height H	ID, Floor number F, Height of floor HF, Volume V, Time T
Slab	Endpoint position	Depth D	ID, Floor number F, Height of floor HF, Volume V, Time T
Column	Column center point	Section size b*h, Height H	ID, Floor number F, Height of floor HF, Volume V, Time T
Beam	Vertical: starting position Horizontal: section center point	Section size b*h, Height H	ID, Floor number F, Height of floor HF, Volume V, Time T
Stairs	Endpoint position	-	ID, Floor number F, Height of floor HF, Volume V, Time T
Roof	Endpoint position	-	ID, Floor number F, Height of floor HF, Volume V, Time T

Table 2. Information required for the calculation of constraints.

Constraint	Required Information	Whether Directly Obtainable from the Parsed BIM Model	Data Required from the BIM Model
Environmental constraint	Outside boundary of a building's first floor	Needs conversion calculation	Coordinates and size of the first floor wall
	Boundary of main road and temporary facilities	Obtained directly	-
Operation constraint	Original and target positions of a lifting component	Needs conversion calculation	Relative position, size, direction, and height of the component
	Weight of the component	Needs conversion calculation	Material and volume of the component
Safety constraint	Height of the building, the outside boundary, and location of a crane jib	Needs conversion calculation	Time, coordinates of slab, wall and column, and location of crane

4.2. Initial Type Selection and Candidate Location Generation

As the selection and localization of mobile cranes are two indispensable steps that cannot be separated independently, an initial crane type should be selected with constraint checks. It means that appropriate cranes need to be re-selected if the initially selected crane type does not meet the constraints. The selection of the crane type mainly considers the maximum lifting weight and the cost of the crane. The weight of a lifting component can be calculated based on its volume and density (see Table 2), which are obtained directly from the IFC format BIM model. After all components C_k required for lift are

traversed, the weights of different components CG_k are compared to determine the maximum weight CG_{max}. Then, CG_{max} and the maximum lifting capacity of the crane G_{max}, which is stored in the crane database, are compared to construct Equation (1). According to the results, all cranes that conform with Equation (1) are added to the alternative crane type database. As for the price, the crane type with the lowest price is selected as the initial crane type to carry out the subsequent calculation of crane localization by assuming G' = hook weight + rigging weight + weight of the other accessories:

$$G_{max} \geq CG_{max} + G' \quad (1)$$

Table 3. Parameter information of a crane required for crane selection and localization.

Constraints/ Optimization	Required Information
Environmental constraint	Outside boundary of a carne after the full extension of legs Rotation radius of the turntable
Operation constraint	Rated lifting weight corresponding to the length and radius of different boom
Minimum lifting time	Boom variation time Maximum elevation of boom Maximum speed of rotation
Lowest price of crane	Market price of crane

The location is determined according to the above three constraints and the optimization conditions. As the safety constraint and efficiency validation are analyzed by traversing each candidate location and simulating the lifting operation, the candidate locations should be represented as a set of discrete points rather than consecutive points in some areas. In this research, the candidate locations of a crane refer to a set of points resulting from the grid method. It divides a construction site into different square grids of the same size, which depends on the size of the crane [21]. The apex of each grid represents the location point of the mobile crane, where the rotation center of the crane is projected to the ground. The position of the point is represented by a three-dimensional Cartesian coordinate system $(x,\ y,\ z)$. The size of the crane can be used as a reference for the width of the grid [26]. If the grid width is less than that of the crane, the adjacent points of the grid point will be covered when the crane is located at a certain point, and the difference between the adjacent points is small. Otherwise, if the width of the grid is larger than that of the crane, it is too sparse for the location of the crane. In addition, the candidate location points also consider the soil condition the crane sits on, where location points with a total load exceeding the land bearing capacity are deleted, which may lead to mobile cranes tipping over.

4.3. Environment Constraint Check

After generating the candidate points, a series of constraints are calculated to gradually remove the points that do not meet the requirements of the candidates; thus, a set of feasible points is obtained. The environmental constraint is tested first to define the boundaries of the buildings, temporary facilities, and main roads in the construction site, and then to eliminate the candidate points where the crane cannot be located to identify its feasible point set FL_1. For the buildings on the construction site, their flat coverage areas can be determined by the location of the ground walls. In IFC format BIM models, the location point of a wall component $(x,\ y,\ z)$ is the starting position of the wall in the longitudinal direction and in the transverse direction. According to the modeling choices in BIM, they may be located at the center line of the wall, that of the core layer, that of the surface layer, the interior/exterior of the surface layer, or that of the core layer. An example is shown in Figure 2. The location point is located exterior to the surface layer, and points A_1 to A_6 are the vertices of the walls W1-W6 of a certain building. For wall W1, the starting point coordinates $A_1(x_1,\ y_1,\ z_1)$, the direction $\vec{R}(a,\ b,\ 0)$, and the length L can be extracted

from the IFC format BIM model, and the line of the wall W1 is expressed by Equation (2). Similarly, the pattern enclosed by the walls W1-W6 is represented by Equation (3):

$$y - y_1 = \frac{b}{a}(x - x_1) \tag{2}$$

$$\begin{cases} y - y_1 = \frac{b}{a}(x - x_1), & x \in (x_1, x_2),\ y \in (y_2, y_1) \\ \cdots\cdots \\ y - y_6 = \frac{b}{a}(x - x_6), & x \in (x_1, x_6),\ y \in (y_1, y_6) \end{cases} \tag{3}$$

where x_i and y_i are the coordinates of the wall Wi.

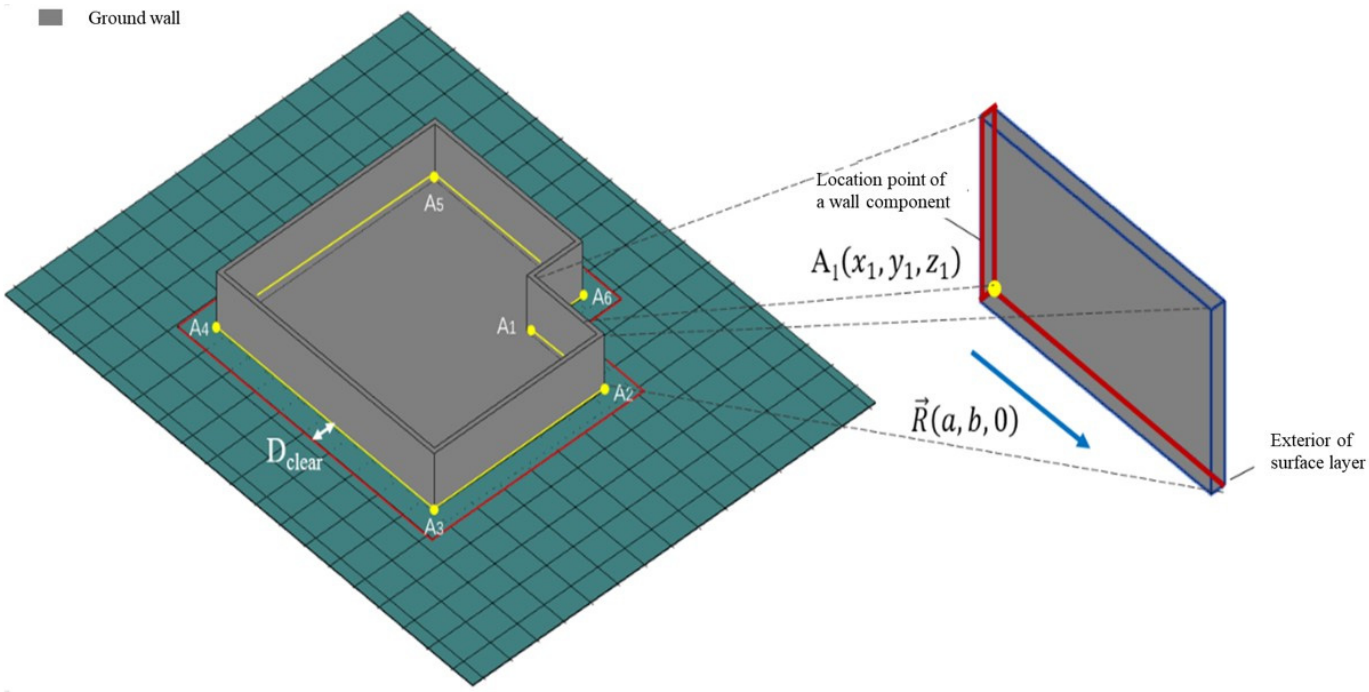


Figure 2. Building coverage area.

Moreover, an initial alternative point represents the rotation center of the crane. Thus, a certain distance from unreachable areas must exist, such as buildings, temporary facilities, and traffic routes, on the construction site. The rotation radius of the turntable is added, with a certain safety distance as the minimum distance D_{clear} between the location point and unreachable areas. The rotation radius of the turntable is determined based on the crane parameters. The safety distance is not specified in the national standard for crane operations. Thus, it can be set as a user's input parameter. The distance from a feasible location point to the nearest unreachable area is calculated. If the distance is less than D_{clear}, the feasible point will be eliminated from the point set.

4.4. Operation Constraint Check

The operation constraint test is carried out to identify whether the selected crane and the feasible alternative points meet the operation requirements. First, the maximum working radius and the maximum boom length of the crane are determined according to the weight of the building components. As shown in Table 4, the rated lifting capacity of the same crane is different under different boom lengths and working radiuses. Due to the limitation of torque, the larger the boom length or the working radius is, the weaker the lifting capacity is. Therefore, according to the original and target positions of the component and the maximum working radius, the location range of the crane can be determined.

Table 4. Lift capacity of a QY100H-3 mobile crane [42,45] (T).

Working Radius (m)	Boom Length (m)								
	13.0	**17.8**	**22.5**	**27.2**	**31.9**	**36.6**	**41.3**	**46.0**	**50.4**
3.0	100	80.0							
3.5	93.0	77.0	62.0						
4.0	88.0	72.0	62.0						
4.5	79.0	67.0	61.0	42.0					
5.0	72.0	62.0	60.0	42.0	40.0				
5.5	65.0	58.0	56.0	42.0	39.0				
6.0	59.0	55.0	52.0	42.0	37.5	31.5			
6.5	54.0	52.0	48.2	40.5	35.8	31.0			
7.0	50.0	49.0	45.0	39.0	34.5	29.5			
7.5	46.0	45.0	42.5	37.0	33.0	28.7			
8.0	42.0	41.0	40.5	35.5	31.8	27.6	23.5		
9.0	36.5	35.5	35.0	32.5	29.5	25.7	22.0	18.5	
10.0	32.0	31.0	30.5	30.0	27.5	24.0	20.8	17.5	
11.0		27.5	26.5	27.5	25.7	22.6	19.5	16.5	14.0
12.0		23.5	23.3	24.5	24.0	21.2	18.9	15.9	13.2
14.0		17.5	17.0	18.5	19.5	18.8	16.9	14.5	12.2
16.0			13.0	14.2	15.0	16.0	15.2	13.2	11.2
18.0			10.0	11.2	12.0	12.6	13.2	12.0	10.2
20.0				9.0	9.7	10.3	10.9	11.0	9.3
22.0				7.2	7.9	8.5	9.0	9.4	8.7
24.0					6.2	7.0	7.6	7.9	8.0
26.0					5.0	5.8	6.3	6.5	6.9
28.0						4.9	5.2	5.6	5.8
30.0						3.9	4.3	4.8	4.9
32.0						3.0	3.6	3.9	4.2
34.0							2.8	3.2	3.6
36.0							2.2	2.7	2.9
38.0								2.2	2.4
40.0								1.8	1.9
42.0									1.6

The maximum working radius R_{max} and the maximum boom length L_{max} of the crane can be automatically determined by the following procedure. From small to large, the rated lifting capacity $G_{m,n}$ corresponding to a different working radius R_n and boom length L_m is invoked and compared with the maximum weight CG_{max} of the lifting components to check whether Equation (4) is satisfied. When $G_{m,n}$ under a certain boom length does not satisfy Equation (4), the comparison between the rated lifting weight of the next level of the boom length and the maximum weight CG_{max} starts, until the comparison of each level of the boom length is conducted. Based on this, the maximum working radius R_{max} and the maximum boom length L_{max} of the crane is determined:

$$G_{m,n} \geq CG_{max} + G', \tag{4}$$

where $G_{m,n}$ is the rated lifting capacity of a crane under a working radius R_n and boom length L_m; and m and n are the level of the boom length and working radius, respectively.

Once the maximum working radius is determined, the plane working range of the crane is also determined. The components whose horizontal distance from the crane is within the maximum working radius can be lifted. Therefore, the distance between the location point of the crane and the original or target position of components should be less than the maximum working radius R_{max}. This research focuses on the prefabricated lifting components; thus, the target position of a lifting component corresponds to its design position in the building model, and its original location is determined by the hoisting scheme, which is presented in the 4D BIM model. Considering that the positions of different components are represented differently in the BIM model, and their target positions

for a crane are represented by their centers of gravity, different coordinate conversions are needed.

1. For a column component, its position coordinates in the BIM model are its bottom center coordinates. Thus, only the z-axis coordinate needs to be re-calculated to determine its target position coordinates. Taking column C_1 as an example, based on its position coordinates $(x_1,\ y_1,\ z_1)$ in the BIM model and its height H and floor height HF obtained from the BIM model, the coordinates of its gravity center are determined as $(x_1,\ y_1,\ HF + H/2)$.
2. For a regular rectangular slab, the coordinates of its gravity center can be calculated from the coordinates of each endpoint of the slab in the model. Taking slab P as an example, based on two diagonal endpoint coordinates $(x_1,\ y_1,\ z_1)$ and $(x_2,\ y_2,\ z_2)$, the height H, the floor height HF, and the slab depth D from the BIM model, the coordinates of its gravity center are $(x_1 + x_2/2,\ (y_1 + y_2)/2,\ HF + H + D/2)$.
3. For wall and beam components in the form of tension, since the position coordinates in the BIM model are the coordinates of the tension starting point, it is necessary to determine the changed plane coordinates of its gravity center. Taking the wall W_1 as an example, based on the starting point coordinates $(x_1,\ y_1,\ z_1)$, direction $\vec{R}(a,\ b,\ 0)$, length L, height H, and floor height HF from the BIM model, the coordinates of its gravity center $(x_1',\ y_1',\ z_1')$ can be calculated using Equation (5):

$$\begin{cases} x_1' = x_1 + \frac{L}{2} \times \frac{a}{\sqrt{a^2+b^2}} \\ y_1' = y_1 + \frac{L}{2} \times \frac{b}{\sqrt{a^2+b^2}} \\ z_1' = HF + \frac{H}{2} \end{cases} \tag{5}$$

After the original and target positions of the building components are determined, for each component C_k to be lifted, its original and target positions are taken, respectively, as the centers of two circles and the maximum working radius R_{max} of the crane is the radius of the circles. As a result, the overlapping area of the two circles is obtained, i.e., the feasible location area of the crane. This is because the distance between any point in the overlapping area and the two centers is less than the maximum working radius of the crane. As an example, Figure 3 shows an intersection for lifting a wall component, involving feasible location points. By following the original feasible point set FL_1, the feasible point set $FL_{2,k}$ for component C_k can be obtained. By traversing all components, the original feasible points that do not belong to any feasible point set $FL_{2,k}$ are eliminated to obtain a feasible point set FL_2. On the other hand, if the two circles do not intersect, meaning that the working radius of the crane does not meet the lifting requirements, the crane needs to be eliminated. Another crane with an increased load capacity would be loaded for the above constraint tests to be performed again.

4.5. Safety Constraint Check

The above two constraint tests screen out the basic feasible location points of the crane based on a 2D plane, which meets the basic requirements, such as accessibility and operability. However, safety problems may exist in crane operations and need to be solved. By traversing all feasible points $FL_{2,k}$ of a component C_k, the collisions between the crane boom and other objects during operation can be identified to prevent safety accidents. The spatial position of the crane boom at the beginning and the end of lifting operations should firstly be determined. For each feasible point of a component C_k, since there are various combinations of boom lengths and working radiuses, to simplify the calculation, the maximum boom length L_{max} obtained in the previous section is selected as its working boom length for calculation. If the maximum boom length does not meet the requirements of the safety constraints, collisions will occur during operations and the relevant location point should be eliminated. If all location points fail to meet the requirements, it means that the crane does not meet the safety requirements. As an example, Figure 4 shows

the position of a lifting boom at the end of lifting work in the plan and space. The plane position can be determined using the plane coordinates of an alternative feasible point P_{ij} (x_i,y_j) and the final position of components (x',y') using Equation (6). In terms of the spatial position, the angle of the boom θ is calculated using the distance between the target position of the component and the feasible location point of the crane and the length of the boom L_{max} based on Equation (7). Moreover, the BIM model is used to obtain construction environment information, including the plane positions of building components when component C_k is lifted at time t_k. Meanwhile, all components', such as beams, columns, walls, and slabs, which might intersect with the crane boom in the plane, maximum heights are selected:

$$ax + by + c = 0, \tag{6}$$

where a, b, and c are constants.

$$\theta = \cos^{-1}\frac{r}{L_{max}}, \tag{7}$$

where $r = \sqrt{(x_i - x')^2 + (y_j - y')^2} + d_{OO'}$; $d_{OO'}$ is the horizontal distance between the rotation center line of the crane boom and the center point of the turntable.

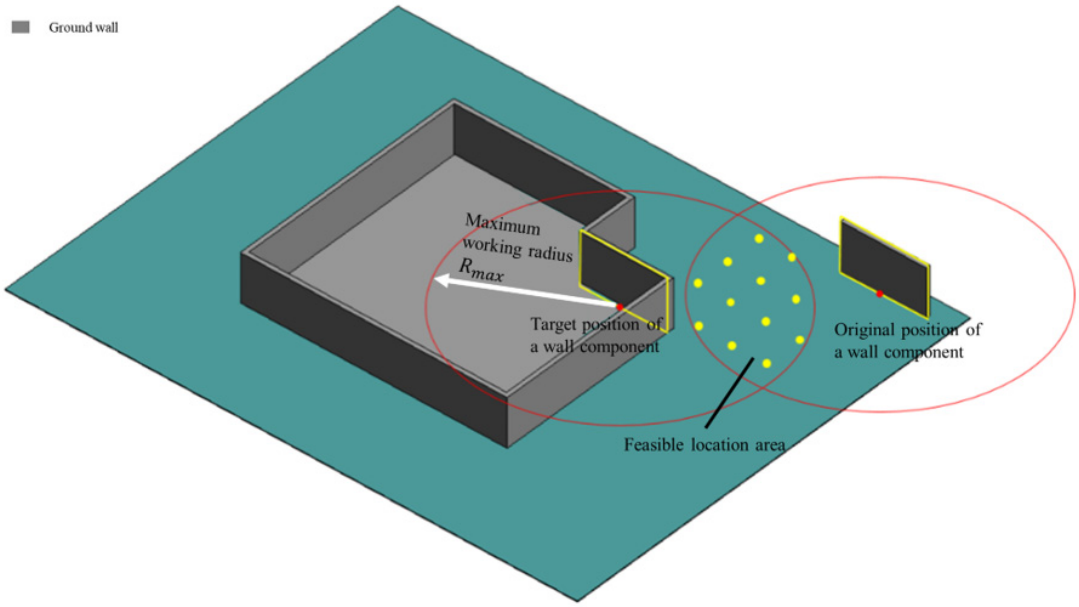


Figure 3. Operation constraint check.

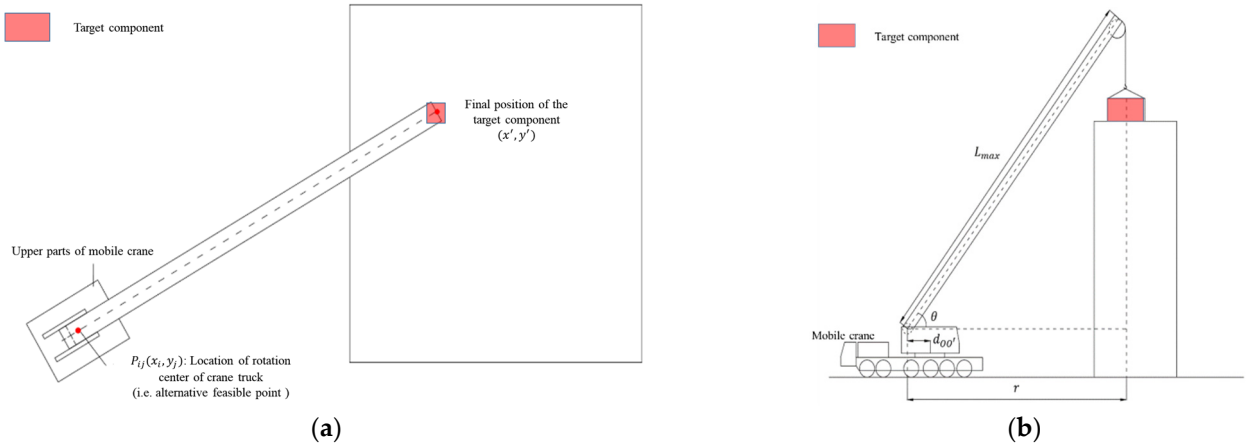


Figure 4. Crane position in the plan and space. (**a**) Lifting boom in the plan, (**b**) Lifting boom in space.

Figure 5 shows an example of the hoist of component C_k. The boom intersects with the exterior wall of the building in the vertical plane at time t. Relevant parameters include the height of the intersection wall H_w, the floor height HF, the coordinates of the starting point of the wall $A_1(x_1, y_1, z_1)$, the direction $\vec{R}(a_1, b_1, 0)$, the wall depth D, and the component height H_c. Assuming that the center line of the wall is the positioning line, the center line of the wall can be expressed by Equation (8). Equations (6) and (8) can be combined to obtain the plane coordinates of the intersection point (x_w, y_w). Then, the plane distance between the location point P_{ij} of the crane and the surface of the wall can be calculated using Equation (9). Finally, Equation (10) is used to identify whether the lifting boom collides with the wall or the component itself. If Equation (10) is satisfied, collisions can be avoided effectively; otherwise, a collision problem will occur. By traversing all feasible points of each component C_k, the above-mentioned safety constraints are calculated to eliminate the points with collisions; thus, the feasible location point set $FL_{3,k}$ is obtained:

$$y - y_1 = \frac{b_1}{a_1}(x - x_1), \tag{8}$$

$$d = \sqrt{(x_i - x_w)^2 + (y_j - y_w)^2} + d_{OO'} - \frac{D}{2\sin\beta}, \tag{9}$$

where $\beta = \tan^{-1}\frac{b}{a} - \tan^{-1}\frac{b_1}{a_1}$.

$$\begin{cases} (d \times \tan\theta + H_{base} - (HF + H_w))\cos\theta \geq d_{clear} \\ (r \times \tan\theta + H_{base} - (HF + H_w + H_c))\cos\theta \geq d_{clear} \end{cases}, \tag{10}$$

where d_{clear} is the minimum distance between the crane boom and the obstacle; H_{base} is the distance between the rotation axis of the crane boom and the ground; and θ is the elevation angle of the boom.

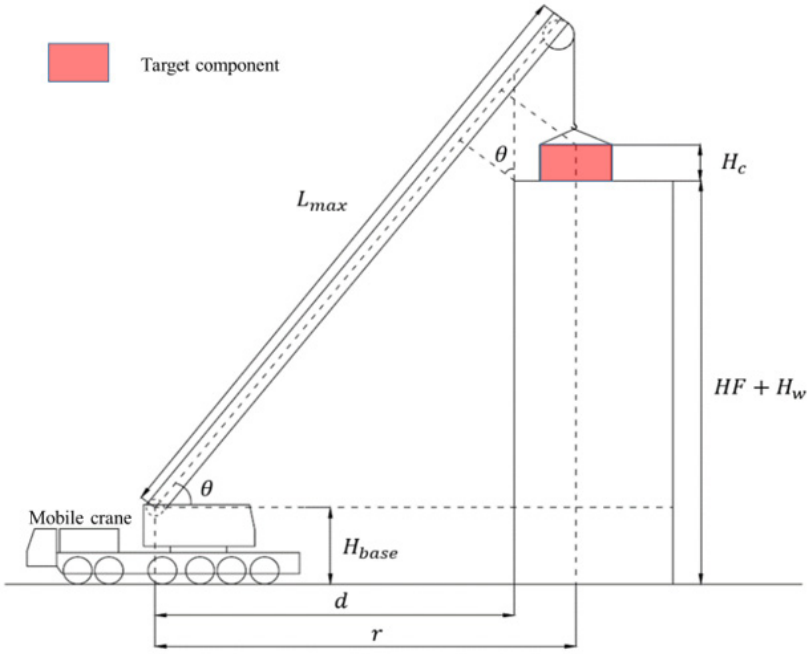


Figure 5. Safety constraint check.

4.6. Lifting Efficiency Optimization

Lifting efficiency is affected by two factors (i.e., the lifting time of a single component and relocation times of a mobile crane). The former consists of the boom variable amplitude time and boom extension time while the latter mainly depends on the lifting schedule stored in 4D BIM.

(1) Minimization of single lifting time

The lifting time of a crane at each location point depends on its work parameters, including the boom variable amplitude time, the boom extension time, the maximum rotation speed, the maximum lifting speed, etc. In a construction site, the boom is preferably stretched without loads, and the lifting height of the hook is independent of the location point and only related to the target installation position of the lifting components. Therefore, the calculation of a single lifting time mainly considers the boom amplitude time and the turntable rotation time. For the point in the feasible point set $FL_{3,k}$ of each component C_k, the boom pitch rotation angle difference $d\theta$ and the turntable rotation angle ω of the crane are firstly calculated. As mentioned above, the initial position coordinates (x_1, y_1, z_1) and final position coordinates (x_2, y_2, z_2) of the component; the boom elevation angles θ_1 and θ_2 of the crane at the beginning and ending operation, respectively; and the position of the lifting boom on the plane $a_1x + b_1y + c_1 = 0$ and $a_2x + b_2y + c_2 = 0$ are obtained. Therefore, the values of $d\theta$ and ω can be calculated using Equations (11) and (12). Then, the lifting time at the point is calculated using Equation (13). The lifting efficiency is calculated successively for several feasible points of the same component and stored in the database:

$$d\theta = |\theta_1 - \theta_2|, \tag{11}$$

$$\omega = \left| \tan^{-1} \frac{b_1}{a_1} - \tan^{-1} \frac{b_2}{a_2} \right| \tag{12}$$

$$T_L = \frac{T_{raising}}{\varphi} \times d\theta + v_{swing} \times \omega, \tag{13}$$

where $T_{raising}$ is the lifting time of the boom; φ is the maximum elevation angle of the lifting boom; and v_{swing} is the rotation speed of the turntable.

(2) Minimization of relocation times

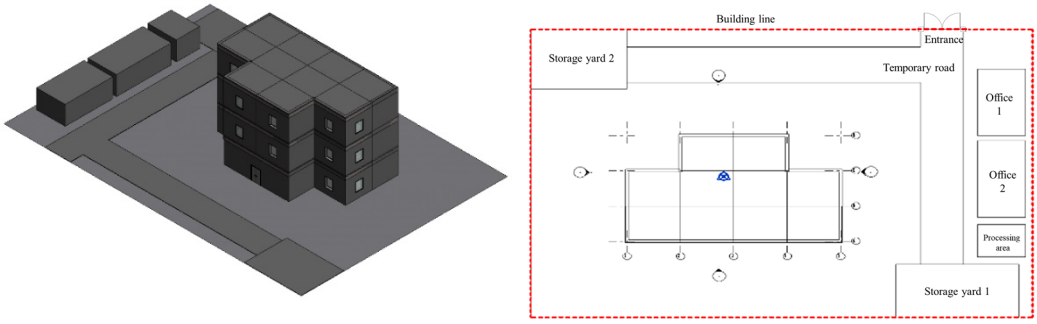
The principle of minimizing relocation times is to find the coincident location points in the feasible points for different lifting components, so that more lifting operations can be performed with the same crane location. It should be noted that due to the complexity of lifting operation, relocation is unavoidable in practical construction even with the minimizing principle. Therefore, according to the lifting schedule, which is stored in 4D BIM, the method used in this research is to iteratively traverse the feasible point set of all components FL_3 and check its attributes. Since the attribute k is added to the feasible point of each component C_k in the operation constraint test, the feasible points with the greatest attribute value is acceptable. The specific procedure is presented as follows.

1. Check the attribute value k of each feasible point P_{ij} in turn, and add points with the same attribute to the same group.
2. Find the group $Group_m$ that contains the most contiguous attributes. Since the attribute value k is the number of components and also represents the lifting order of components, the lifting order should be considered to ensure that the attribute value is as continuous as possible.
3. Compare the minimum lifting time when the crane is located at the points of multiple $Group_m$, and select the group with the shortest lifting time as the final $Group_m$. If no multiple $Group_m$ exist, go straight to the next step.
4. Take point $P_{ij,k}$ in $\mathrm{Group_m}$ as the location point of the crane for the hoist of the component C_k, and release the attribute value k contained in other points at the same time.
5. Identify the remaining feasible point with the greatest attribute k and repeat the above steps.
6. Identify the crane location point combinations with the minimum number of movements after completing the above steps for all feasible points, calculate the lifting time of each point in the same group of location points, and take the point combination with the shortest lifting time.

Through the above steps, the optimal location point of the mobile crane with minimum relocations and the shortest lifting time can be identified.

5. Case Study

To test the feasibility and validity of the proposed method, a crane selection and localization system were developed based on Unity 3D, including the input module, selection module, positioning module, and optimization module, and a case of a 3-story prefabricated building project was adopted, involving the integrated selection and localization of a mobile crane under a lifting scenario of multi-components. In this case, the BIM model of the building was constructed in advance, with various types of precast components (see Figure 6a). In addition, site roads, temporary facilities, and relevant coordinates were directly extracted from the parsed IFC format BIM model, marked in the construction site layout (see Figure 6b). Table 5 lists some candidate mobile cranes and their basic performances stored in the crane database.



(**a**) (**b**)

Figure 6. BIM model and site layout (**a**) BIM model of the building with precast components. (**b**) Roads and temporary facilities in the construction site layout.

Table 5. Basic performances of the candidate cranes in the database.

Crane Model	Maximum Lifting Capacity (T)	Maximum Boom Length (m)	Maximum Working Radius (m)	Cost (Yuan/per Machine)
QY16D	16	30.5	22	1100
QY20G	20	32.27	28	1360
QY25K-I	25	33	30	1800
QY50K-II	50	42.7	32	2960
QY65K	65	42	30	3500
QY70K	70	44.5	36	4780
QY80K	80	45	36	5000
QY90K	90	55	50	5800
QY100K-I	100	51	42	6833
QY130K	130	58	56	6900
QY160K	160	62	52	7000

5.1. Data Input

The IFC format BIM model was firstly imported into the system using its input module to automatically obtain the attributes of all precast components, and the coordinates of the obstacles and stacking yards in the construction site. Referring to the range of building, facilities, and site, an initial candidate location point set for the mobile crane was generated automatically to support the subsequent selection and localization of the crane.

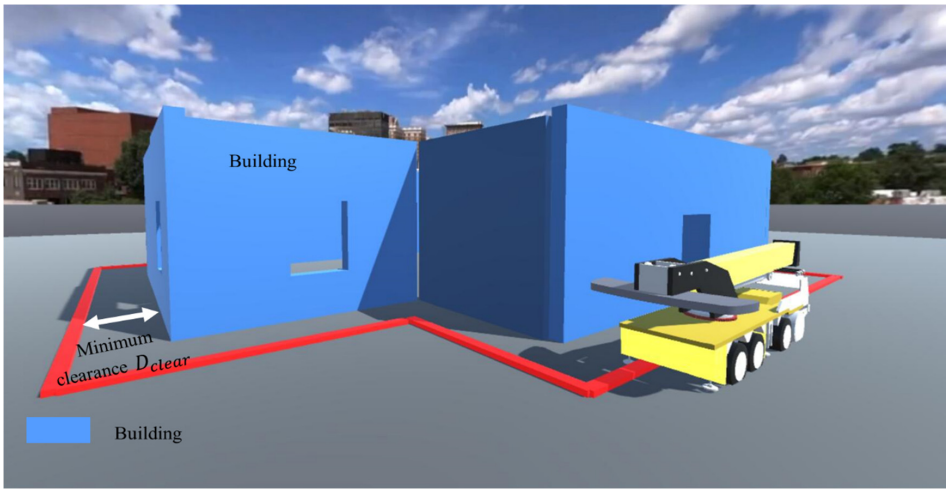
5.2. Initial Crane Type Selection

According to the maximum weight of the precast components, 4 types of mobile cranes were selected based on Equation (1), including QY90K, QY100K-I, QY130K, and

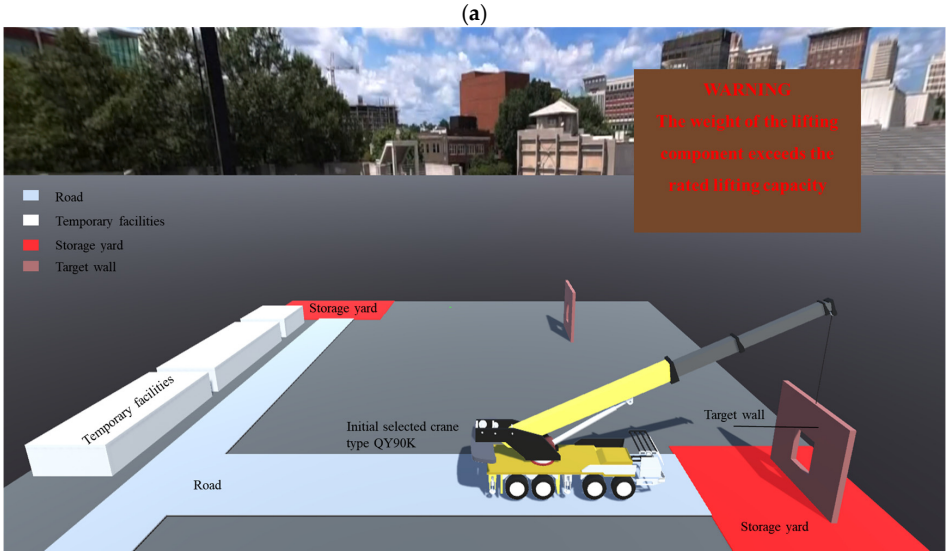
QY160K, and added to the alternatives. QY90K was automatically selected as the initial crane type by the selection module because of its lowest price. Then, the performance parameters of the selected mobile crane were extracted from the crane database to support the subsequent calculation.

5.3. Constraint Checks

The environmental constraint check, operation constraint check, and safety constraint check were performed orderly using the positioning module to check the feasibility of the selected crane type. The points satisfying the three constraints were set as the feasible location points, which meant these components could be hoisted safely. However, it was found that in terms of the initial crane type QY90K, all constraints with the lifting components could not be satisfied. Thus, the crane type had to be eliminated from the alternatives. Figure 7 shows the scenarios in which crane QY90K was inconsistent with the three constraints. Specifically, Figure 7a shows the crane was located within the boundaries of the existing buildings, which is defined by the minimum clearance, Figure 7b shows the weight of the lifting component that exceeded the rated lifting capacity, and Figure 7c shows there was a collision between the crane boom and the building during lifting operation. Another alternative crane type QY100K-I with the minimum cost was loaded as a new initial type for repeated constraint testing. As a result, this crane type conformed with all of the constraints, and the feasible location points were obtained (see Figure 8).

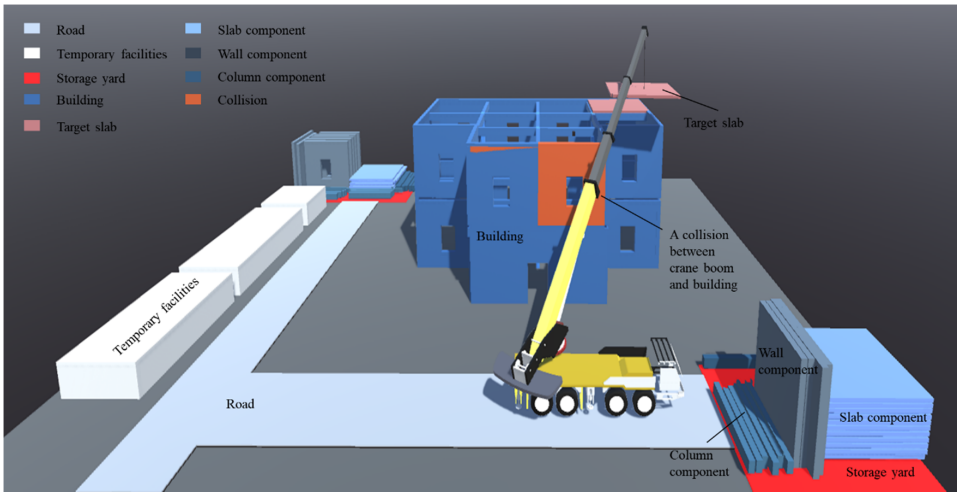


(**a**)



(**b**)

Figure 7. *Cont.*



(**c**)

Figure 7. The initially selected type QY90K, which does not satisfy the constraints. (**a**) Unsatisfied environmental constraint. (**b**) Unsatisfied operation constraint. (**c**) Unsatisfied safety constraint.

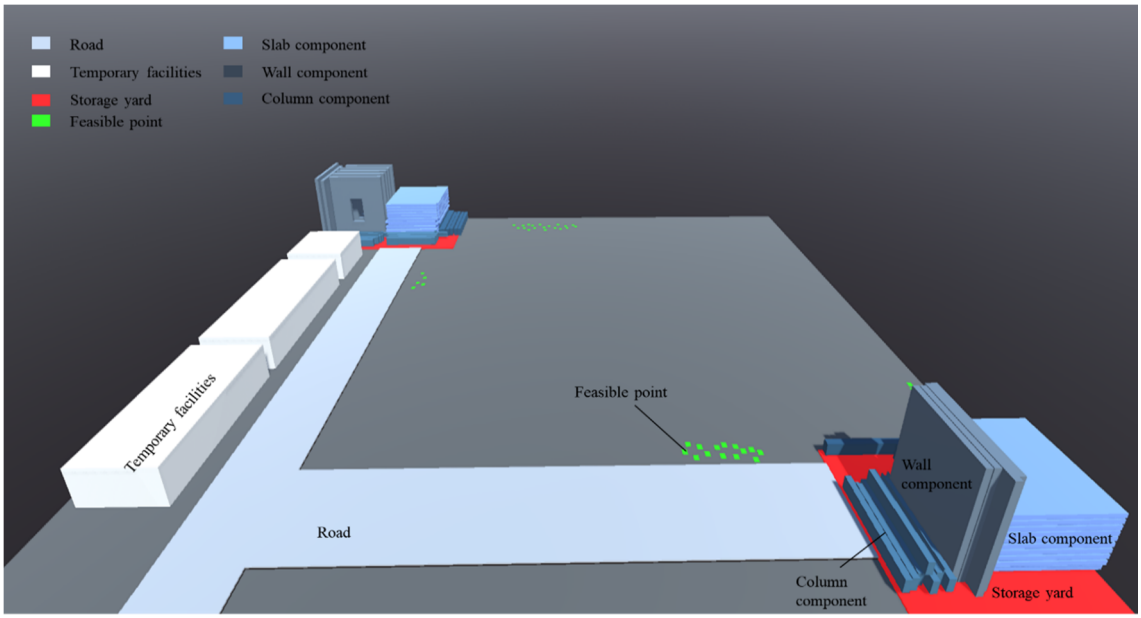


Figure 8. Feasible location points for a certain component (crane type QY100K-I).

5.4. Optimal Combination of Feasible Location Points

Based on the obtained feasible points for all lifting components, the combination with the minimum relocations of 2 (i.e., the optimal location point 1 and 2 in Figure 9) and the shortest lifting time was determined using the optimization module. The optimal locations were highlighted in the construction site layout. As shown in Figure 9, the highlighted combination of feasible points represents the optimal locations for the selected mobile crane QY100K-I.

It is shown from this case study that the proposed method is workable. Moreover, the selection and localization processes of the mobile crane can be automatically conducted by the developed system. Thus, it makes the selection and localization of the mobile crane more efficient than before, not only saving cost and time but also improving the safety performance. Furthermore, this proposed method has the potential to support the automatic simulation of construction processes, which further supports the implementation of intelligent construction.

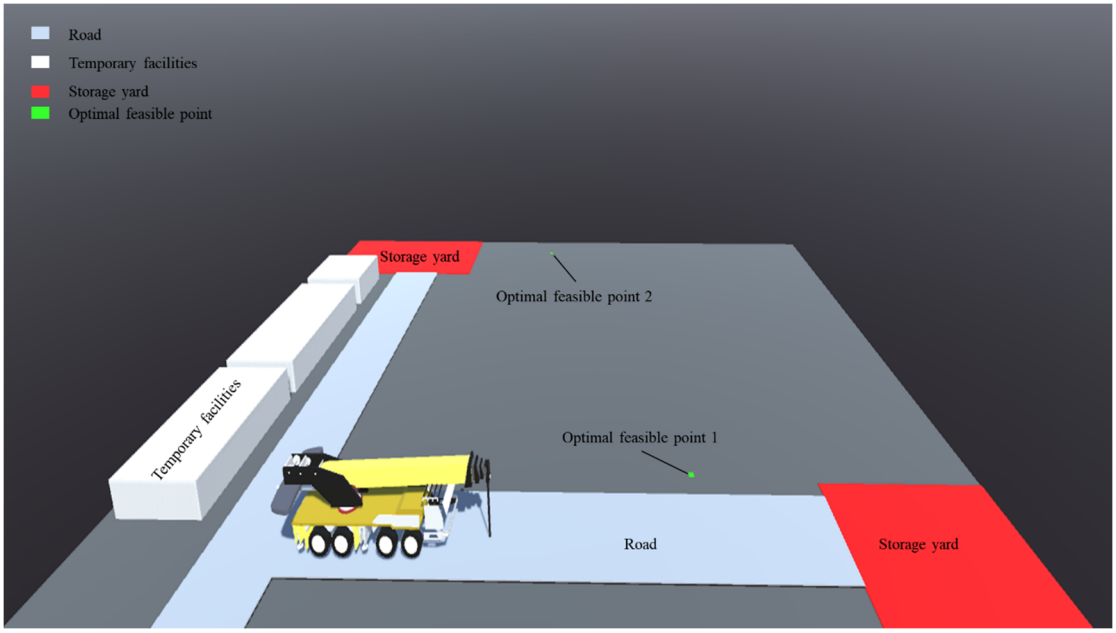


Figure 9. Optimal combination of feasible location points for crane QY100K-I.

6. Conclusions

The promotion of virtual construction technologies has the potential to improve the efficiency and safety of crane operation by producing a more precise, comprehensive, and dynamic operation plan. However, in terms of the selection and localization of the mobile crane, it seldom considers the combination of different feasible location points, the minimization of crane movement, and the spatial safety requirements during lifting processes. Consequently, this study developed a method to automatically select and locate the mobile crane, mainly involving three constraints, i.e., the environmental constraint, operation constraint, and safety constraint, and two optimization methods covering the least cost, minimum relocations, and shortest lifting time. Relevant parameter information can be directly obtained or indirectly transformed from the 4D BIM model. A case study was also presented to test the feasibility and validity of the proposed method. The result shows that the method was feasible and valid in the virtual simulation environment. This benefits not only on-site crane operations but also automatic construction simulation. Moreover, compared with other construction machinery, mobile cranes have more constraints and more complicated operation. Thus, it is easier to extend the method to other construction machinery.

In addition, there are still some limitations. On the one hand, the proposed method was only tested in a virtual construction scenario and the optimized result has not yet been used in real construction. On the other hand, the method only considered the construction scenario with a single mobile crane. Thus, future research will focus on the use of optimized results from the method in real construction scenarios to test its performance, with more criteria (i.e., wind effect, ground bearing pressure, and rope breakage) considered. Moreover, multi-crane construction scenarios will also be taken into consideration in the future.

Author Contributions: Conceptualization, H.G. and Y.Y.; methodology, Y.Z. and Z.P.; validation, Y.L. and Z.Z.; formal analysis, Z.Z.; investigation, Y.Z.; writing—original draft preparation, H.G. and Y.Z.; writing—review and editing, Y.Y. and Y.Z.; visualization, Y.Z. and Y.Y.; supervision, H.G. and Y.Y.; project administration, H.G.; funding acquisition, H.G. All authors have read and agreed to the published version of the manuscript.

Funding: This research was funded by the National Natural Science Foundation of China, grant number 51578318 and 51208282.

Institutional Review Board Statement: Not applicable.

Informed Consent Statement: Not applicable.

Data Availability Statement: Some or all data, models, or code that support the findings of this study are available from the corresponding author upon reasonable request.

Acknowledgments: We would like to thank Tsinghua-Glodon BIM Research Center for supporting this research. This paper is an extension of a conference paper "*Automated Method for Optimizing Feasible Locations of Mobile Cranes Based on 3D Visualization*" [42] in Creative Construction Conference (CCC) 2017.

Conflicts of Interest: The authors declare no conflict of interest.

References

1. Kang, S.; Miranda, E. Planning and visualization for automated robotic crane erection processes in construction. *Autom. Constr.* **2006**, *15*, 398–414. [CrossRef]
2. Lacey, A.; Chen, W.; Hao, H.; Bi, K. Structural response of modular buildings–An overview. *J. Build. Eng.* **2018**, *16*, 45–56. [CrossRef]
3. Olearczyk, J.; Al-Hussein, M.; Bouferguene, A.; Telyas, A. 3D-Modeling for Crane Selection and Logistics for Modular Construction On-Site Assembly. In *Computing in Civil Engineering*; ASCE: Reston, VA, USA, 2012. [CrossRef]
4. Olearczyk, J.; Al-Hussein, M.; Bouferguène, A. Evolution of the crane selection and on-site utilization process for modular construction multilifts. *Autom. Constr.* **2014**, *43*, 59–72. [CrossRef]
5. Lei, Z.; Han, S.; Bouferguene, A.; Taghaddos, H.; Hermann, U.; Al-Hussein, M. Algorithm for Mobile Crane Walking Path Planning in Congested Industrial Plants. *J. Constr. Eng. Manag.* **2015**, *141*, 05014016. [CrossRef]
6. Lin, Y.; Yu, H.; Sun, G.; Shi, P. Lift Path Planning without Prior Picking/Placing Configurations: Using Crane Location Regions. *J. Comput. Civ. Eng.* **2016**, *30*, 04014109. [CrossRef]
7. Kang, S.; Miranda, E. Computational methods for coordinating multipole construction cranes. *J. Comput. Civ. Eng.* **2008**, *22*, 252–263. [CrossRef]
8. Fang, Y.; Teizer, J. A Multi-User Virtual 3D Training Environment to Advance Collaboration Among Crane Operator and Ground Personnel in Blind Lifts. In *Computing in Civil and Building Engineering*; ASCE: Reston, VA, USA, 2014. [CrossRef]
9. Chen, Y.-C.; Chi, H.-L.; Kang, S.-C.; Hsieh, S.-H. Attention-Based User Interface Design for a Tele-Operated Crane. *J. Comput. Civ. Eng.* **2016**, *30*, 04015030. [CrossRef]
10. Al-Hussein, M.; Niaz, M.A.; Yu, H.; Kim, H. Integrating 3D visualization and simulation for tower crane operations on construction sites. *Autom. Constr.* **2006**, *15*, 554–562. [CrossRef]
11. Mara, T.G. Effects of a Construction Tower Crane on the Wind Loading of a High-Rise Building. *J. Struct. Eng.* **2010**, *136*, 1453–1460. [CrossRef]
12. Ali, G.M.; Kosa, J.; Bouferguene, A.; Al-Hussein, M. Competitive Assessment of Ice and Frozen Silt Mat for Crane Ground Support Using Finite-Element Analysis. *J. Constr. Eng. Manag.* **2021**, *147*, 04021038. [CrossRef]
13. Ali, G.M.; Olearczyk, J.; Bouferguene, A.; Al-Hussein, M. Implementation of Combined Loading to Calculate Ground Bearing Pressure under Crawler Crane Tracks. *J. Constr. Eng. Manag.* **2021**, *147*, 04021051. [CrossRef]
14. Yu, G.Y.H. Forensic investigation on crane accidents. *Int. J. Forensic Eng.* **2017**, *3*, 319–341. [CrossRef]
15. Wang, R.D.; Zayed, T.; Pan, W.; Zheng, S.; Tariq, S. A system boundary-based critical review on crane selection in building construction. *Autom. Constr.* **2020**, *123*, 103520. [CrossRef]
16. Al-Hussein, M.; Alkass, S.; Moselhi, O. An algorithm for mobile crane selection and location on construction sites. *Constr. Innov.* **2001**, *1*, 91–105. [CrossRef]
17. Moselhi, O.; Alkass, S.; Al-Hussein, M. Innovative 3D-modelling for selecting and locating mobile cranes. *Eng. Constr. Arch. Manag.* **2004**, *11*, 373–380. [CrossRef]
18. Al-Hussein, M.; Alkass, S.; Moselhi, O. Optimization Algorithm for Selection and on Site Location of Mobile Cranes. *J. Constr. Eng. Manag.* **2005**, *131*, 579–590. [CrossRef]
19. Wu, D.; Lin, Y.; Wang, X.; Wang, X.; Gao, S. Algorithm of Crane Selection for Heavy Lifts. *J. Comput. Civ. Eng.* **2011**, *25*, 57–65. [CrossRef]
20. Hasan, S.; Al-Hussein, M.; Hermann, U.H.; Safouhi, H. Interactive and Dynamic Integrated Module for Mobile Cranes Supporting System Design. *J. Constr. Eng. Manag.* **2010**, *136*, 179–186. [CrossRef]
21. Han, S.H.; Hasan, S.; Bouferguène, A.; Al-Hussein, M.; Kosa, J. Utilization of 3D Visualization of Mobile Crane Operations for Modular Construction On-Site Assembly. *J. Manag. Eng.* **2015**, *31*, 04014080. [CrossRef]
22. Han, S.; Al-Hussein, M.; Hasan, S.; Gökçe, K.U.; Bouferguene, A. Simulation of mobile crane operations in 3D space. In Proceedings of the 2012 Winter Simulation Conference, Berlin, Germany, 9–12 December 2012.
23. Furusaka, S.; Gray, C. A model for the selection of the optimum crane for construction sites. *Constr. Manag. Econ.* **1984**, *2*, 157–176. [CrossRef]
24. Han, S.; Bouferguene, A.; Al-Hussein, M.; Hermann, U. 3D-based crane evaluation system for mobile crane operation selection on mod-ular-based heavy construction sites. *J. Constr. Eng. Manag.* **2017**, *143*, 04017060. [CrossRef]

25. Zaki, T.M.; Hosny, O.; Nassar, K. An automated model for selecting the optimum mobile crane model and on-site position using genetic algorithms. In Proceedings of the Canadian Society for Civil Engineering's 5th International/11th Construction Specialty Conference, Vancouver, BC, Canada, 8–10 June 2015; p. 128.
26. Taghaddos, H.; AbouRizk, S.; Mohamed, Y.; Hermann, U. Simulation-Based Multiple Heavy Lift Planning in Industrial Construction. In *Construction Research Congress*; ASCE: Reston, VA, USA, 2010; pp. 349–358. [CrossRef]
27. Raynar, K.A.; Smith, G.R. Intelligent Positioning of Mobile Cranes for Steel Erection. *Comput. Civ. Infrastruct. Eng.* **1993**, *8*, 67–74. [CrossRef]
28. Tantisevi, K.; Akinci, B. Simulation-Based Identification of Possible Locations for Mobile Cranes on Construction Sites. *J. Comput. Civ. Eng.* **2008**, *22*, 21–30. [CrossRef]
29. Lei, Z.; Taghaddos, H.; Olearczyk, J.; Al-Hussein, M.; Hermann, U. Automated Method for Checking Crane Paths for Heavy Lifts in Industrial Projects. *J. Constr. Eng. Manag.* **2013**, *139*, 04013011. [CrossRef]
30. Ding, L.; Zhou, Y.; Akinci, B. Building Information Modeling (BIM) application framework: The process of expanding from 3D to computable nD. *Autom. Constr.* **2014**, *46*, 82–93. [CrossRef]
31. Hermann, U.; Hendi, A.; Olearczyk, J.; Al-Hussein, M. An Integrated System to Select, Position, and Simulate Mobile Cranes for Complex Industrial Projects. In Proceedings of the Construction Research Congress 2010, Banff, AB, Canada, 8–10 May 2010; pp. 267–276.
32. Han, S.; Lei, Z.; Bouferguene, A.; Al-Hussein, M.; Hermann, U. 3D Visualization-Based Motion Planning of Mobile Crane Operations in Heavy Industrial Projects. *J. Comput. Civ. Eng.* **2016**, *30*, 04014127. [CrossRef]
33. Kang, S.; Miranda, E. Numerical methods to simulate and visualize detailed crane ctivities. *Comput. Aided Civ. Infrastruct. Eng.* **2009**, *24*, 169–185. [CrossRef]
34. Tantisevi, K.; Akinci, B. Automated generation of workspace requirements of mobile crane operations to support conflict de-tection. *Autom. Constr.* **2007**, *16*, 262–276. [CrossRef]
35. Wang, X.; Liu, J.; Liu, F.; Gao, S. Collision-free locating of mobile cranes in 3D lifting system. In Proceedings of the ASME 2010 International Design Engineering Technical Conferences and Computers and Information in Engineering Conference, Montreal, QC, Canada, 15–18 August 2010; pp. 479–486.
36. Zi, B.; Lin, J.; Qian, S. Localization, obstacle avoidance planning and control of a cooperative cable parallel robot for multiple mobile cranes. *Robot. Comput. Manuf.* **2015**, *34*, 105–123. [CrossRef]
37. Ji, Y.; Leite, F. Optimized planning approach for multiple tower cranes and material supply points using mixed-integer programming. *J. Constr. Eng. Manag.* **2020**, *146*, 04020007. [CrossRef]
38. Briskorn, D.; Dienstknecht, M. Mixed-integer programming models for tower crane selection and positioning with respect to mutual interference. *Eur. J. Oper. Res.* **2018**, *273*, 160–174. [CrossRef]
39. Yeoh, J.K.W.; Chua, D.K.H. Optimizing Crane Selection and Location for Multistage Construction Using a Four-Dimensional Set Cover Approach. *J. Constr. Eng. Manag.* **2017**, *143*, 04017029. [CrossRef]
40. Lin, J.; Fu, Y.; Li, R.; Lai, W. An Algorithm for Optimizing the Location and Type Selection of Attached Tower Cranes Based on Value Engineering. In *ICCREM 2020: Intelligent Construction and Sustainable Buildings*; ASCE: Reston, VA, USA, 2020; pp. 106–117. [CrossRef]
41. Yoon, S.; Park, M.; Jung, M.; Hyun, H.; Ahn, S. Multi-objective optimization model for tower crane layout planning in modular con-struction. *Korean J. Constr. Eng. Manag.* **2021**, *22*, 36–46.
42. Pan, Z.; Guo, H.; Li, Y. Automated Method for Optimizing Feasible Locations of Mobile Cranes Based on 3D Visualization. *Procedia Eng.* **2017**, *196*, 36–44. [CrossRef]
43. Zhou, Y.; Guo, H.; Ma, L.; Zhang, Z.; Skitmore, M. Image-based onsite object recognition for automatic crane lifting tasks. *Autom. Constr.* **2020**, *123*, 103527. [CrossRef]
44. Hongling, G.; Ying, Z.; Xiaotian, Y.; Zhubang, L.; Fan, X. Automated mapping from an IFC data model to a relational database model. *J. Tsinghua Univ.* **2021**, *61*, 152–160.
45. Available online: https://cn.auto-che.com/b/puyuan/truck-crane.html (accessed on 22 March 2022).